

Transformation of a Mismatched Nonlinear Dynamic System into Strict Feedback Form

Johanna L. Mathieu¹

Mem. ASME
e-mail: jmathieu@berkeley.edu

J. Karl Hedrick

Professor
ASME Fellow
e-mail: khedrick@me.berkeley.edu

Department of Mechanical Engineering,
University of California, Berkeley,
6141 Etcheverry Hall, MC 1740,
Berkeley, CA 94720

Dynamic surface control is a robust nonlinear control technique. It is generally applied to mismatched dynamic systems in strict feedback form. We have developed a new method of defining states and state-dependent disturbances to transform a mismatched dynamic system into strict feedback form. We apply this method to a multi-input multi-output (MIMO) extended-state kinematic model of a bicycle. We show how a dynamic surface controller can be used for position tracking of the bicycle. The performance of the dynamic surface controller is compared with that of a controller designed using feedback linearization. Transformation of the dynamic system into strict feedback form allows us to successfully apply dynamic surface control. Both the dynamic surface controller and the feedback linearization controller perform well in the absence of disturbances. The dynamic surface controller is more robust when disturbances are introduced; however, a large control effort is required to reject the disturbances. Our method of defining new states and state-dependent disturbances to transform mismatched nonlinear dynamic systems into strict feedback form could be used on other systems requiring robust nonlinear control.

[DOI: 10.1115/1.4003795]

Keywords: strict feedback form, mismatched system, nonlinear control, dynamic surface control, feedback linearization, bicycle

1 Introduction

Nonlinear control techniques are an obvious choice when system linearization yields uncontrollable linear models. Two common methods for controlling nonlinear systems are feedback linearization (FL) and sliding control [1]. Feedback linearization is a way of simplifying nonlinear controller design by transforming original system models into equivalent models that can be controlled with linear techniques. While effective at controlling systems with precise models (and precise derivatives of those models), feedback linearization is not robust with respect to model uncertainty. Sliding control is a more robust method for controlling nonlinear systems. Traditional techniques for sliding control, as presented in Ref. [1], work well for systems that satisfy the “matching condition” [2], meaning that a control exists in each channel with uncertainty; however, these techniques do not work for mismatched systems because they would require bounding the derivative of the uncertainty, an impossible task. Alternative techniques, which avoid this problem, include integrator backstepping [2] and using multiple sliding surfaces [3]. However, these techniques lead to an “explosion of terms” [4].

Dynamic surface control (DSC), as described in Ref. [4], is a robust technique used to control mismatched nonlinear systems. The method employs low-pass filters that introduce a delay (and therefore error) in exchange for avoiding an “explosion of terms.” DSC has been used to control many different types of systems including remotely operated underwater vehicles [5], automated cars [6], and ships [7].

DSC is generally applied to mismatched dynamic systems in strict feedback form [4], a subset of semistrict feedback form [8,9]. In this paper, we present a new method of defining states

and state-dependent disturbances to transform a mismatched dynamic system into strict feedback form. We apply this method to a nonlinear, multi-input multi-output (MIMO), extended-state, mismatched, kinematic model of a bicycle. Our goal is for the bicycle to track a desired trajectory, a control objective that has been explored by many researchers (e.g., Refs. [10–12]). The bicycle model and variations on it have also been used to design steer-by-wire controllers for automobiles, by ignoring the roll degree of freedom (e.g., Refs. [13,14]). To demonstrate the robustness of the dynamic surface controller, we compare its performance to that of a controller designed using feedback linearization. Note that an earlier version of this paper was presented at the 2010 American Controls Conference [15].

The following section includes a description of the system, the dynamic model, and the controllability analysis. Section 3 describes the design of a controller using feedback linearization. Section 4 describes the method of defining states and state-dependent disturbances to transform the system into strict feedback form, and the design of a dynamic surface controller. Section 5 presents simulation results, and Section 6 concludes.

2 Dynamic System Description and Controllability

A bicycle can be modeled as a four state system, as illustrated in Fig. 1. The states are as follows: x_1 is the distance in x to the back wheel (with respect to a fixed coordinate system), x_2 is the distance in y to the back wheel (with respect to the same fixed coordinate system), ψ_1 is the heading angle (angle between the bicycle axis and the x axis), and ψ_2 is the steering angle (angle between axis of the front wheel and the bicycle axis).

The rider controls the forward velocity of the bicycle and the angular velocity of the handle bars. Therefore, the following two inputs are used: u_1 is the forward velocity of the bicycle and u_2 is the angular velocity of the handle bars.

The kinematic relations governing the motion of the bicycle are as follows:

$$\dot{x}_1 = \cos(\psi_1 + \psi_2)u_1 \quad (1)$$

¹Corresponding author.

Contributed by the Dynamic Systems, Measurement and Control Division of ASME for publication in the JOURNAL OF DYNAMIC SYSTEMS, MEASUREMENT, AND CONTROL. Manuscript received July 23, 2010; final manuscript received January 12, 2011; published online April 11, 2011. Assoc. Editor: Marcio de Queiroz.

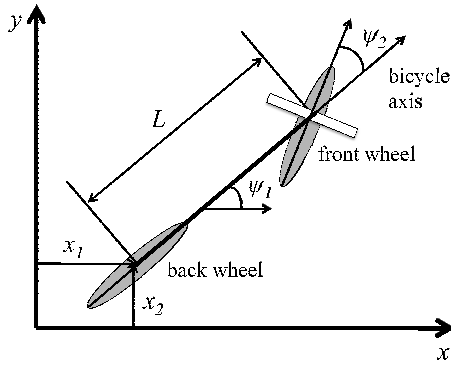


Fig. 1 Geometry of a bicycle

$$\dot{x}_2 = \sin(\psi_1 + \psi_2)u_1 \quad (2)$$

$$\dot{\psi}_1 = \frac{\sin(\psi_2)u_1}{L} \quad (3)$$

$$\dot{\psi}_2 = u_2 \quad (4)$$

The first two state equations, specifying the velocity of the bicycle's back wheel in x and y , are derived from geometry. The third state equation, which defines how the steering angle affects the heading angular velocity, is given in Ref. [16]. Here, $\sin(\psi_2)u_1$ is the velocity of the bicycle perpendicular to the bicycle axis and L , the distance between the wheel axles, is the radius of the turn. The fourth state equation results from the inability of the rider to control the position of the handle bars directly; instead, the rider controls the angular velocity of the handle bars.

We set

$$\alpha = \frac{\sin(\psi_2)}{L} \quad (5)$$

where α is a parameter characterizing the steering angle. A bicycle's steering angle, ψ_2 , is small and we normalize L to 1 so $\alpha \cong \psi_2$. Also, $\psi_1 \gg \psi_2$ so $\psi_1 + \psi_2 \cong \psi_1$. For simplicity, we set $\psi = \psi_1$. The simplified state equations are

$$\dot{x}_1 = \cos(\psi)u_1 \quad (6)$$

$$\dot{x}_2 = \sin(\psi)u_1 \quad (7)$$

$$\dot{\psi} = \alpha u_1 \quad (8)$$

$$\dot{\alpha} = u_2 \quad (9)$$

For the purpose of this analysis, the output equation is defined as the position of the back wheel, which we assume we can measure directly

$$y = \begin{bmatrix} y_1 \\ y_2 \end{bmatrix} = \begin{bmatrix} x_1 \\ x_2 \end{bmatrix} \quad (10)$$

Written in standard form, the nonlinear system can be expressed as

$$\dot{x} = f(x) + g_1(x)u_1 + g_2(x)u_2 \quad (11)$$

where $f(x)=0$,

$$x = \begin{bmatrix} x_1 \\ x_2 \\ \psi \\ \alpha \end{bmatrix}, \quad g_1(x) = \begin{bmatrix} \cos(\psi) \\ \sin(\psi) \\ \alpha \\ 0 \end{bmatrix}, \quad \text{and} \quad g_2(x) = \begin{bmatrix} 0 \\ 0 \\ 0 \\ 1 \end{bmatrix}$$

To determine the accessibility [17] of the full MIMO nonlinear system, we form the accessibility matrix:

$$C = [g_1, g_2, [g_1, g_2], [g_1, [g_1, g_2]]] = \begin{bmatrix} \cos(\psi) & 0 & 0 & -\sin(\psi) \\ \sin(\psi) & 0 & 0 & \cos(\psi) \\ \alpha & 0 & 1 & 0 \\ 0 & 1 & 0 & 0 \end{bmatrix} \quad (12)$$

where $[g_1, g_2]$ is the Lie bracket between g_1 and g_2 . We find that $\det(C)=-1$. C is full rank for all values of ψ and α so the system is locally accessible everywhere. Moreover, since $f(x)=0$, the system is controllable [18]. This means that for any initial state and any target state, there exists a control function that will transfer the bicycle from the initial state to the target state in finite time.

3 Control Using Feedback Linearization

MIMO input/output feedback linearization of this system is achieved through use of dynamic extension [2,17,18], which requires the definition of new states corresponding to inputs of the original system. Ultimately, dynamic extension allows us to decouple the derivatives of the rows of the output equation, which we will set equal to a synthetic input, allowing us to solve for the control input.

To illustrate the need to use dynamic extension, we first differentiate the output equation (10) until the control explicitly appears:

$$\dot{y} = l_1 + J_1 \begin{bmatrix} u_1 \\ u_2 \end{bmatrix} \quad (13)$$

where $l_1=0$ and J_1 is the decoupling matrix:

$$J_1 = \begin{bmatrix} \cos(\psi) & 0 \\ \sin(\psi) & 0 \end{bmatrix} \quad (14)$$

Unfortunately, J_1 is singular so the two equations cannot be decoupled.

Using dynamic extension, we define a new state $x_3=u_1$ and its derivative $\dot{x}_3=u_3$, where u_3 controls the acceleration of the bicycle. We now have a redefined system with five states:

$$\dot{x}_1 = \cos(\psi)x_3 \quad (15)$$

$$\dot{x}_2 = \sin(\psi)x_3 \quad (16)$$

$$\dot{\psi}_1 = \alpha x_3 \quad (17)$$

$$\dot{\alpha} = u_2 \quad (18)$$

$$\dot{x}_3 = u_3 \quad (19)$$

Differentiating Eq. (10) until the control explicitly appears yields

$$\ddot{y} = l_2 + J_2 \begin{bmatrix} u_2 \\ u_3 \end{bmatrix} \quad (20)$$

where l_2 is a function of the states and J_2 is the new decoupling matrix:

$$J_2 = \begin{bmatrix} 0 & \cos(\psi) \\ 0 & \sin(\psi) \end{bmatrix} \quad (21)$$

Unfortunately, J_2 is also singular so we apply dynamic extension again and define a second new state $x_4=u_3$ and its derivative $\dot{x}_4=u_4$, where u_4 controls the jerk of the bicycle. We now have a redefined system with six states:

$$\dot{x}_1 = \cos(\psi)x_3 \quad (22)$$

$$\dot{x}_2 = \sin(\psi)x_3 \quad (23)$$

$$\dot{\psi}_1 = \alpha x_3 \quad (24)$$

$$\dot{\alpha} = u_2 \quad (25)$$

$$\dot{x}_3 = x_4 \quad (26)$$

$$\dot{x}_4 = u_4 \quad (27)$$

Differentiating Eq. (10) until the control explicitly appears yields

$$\ddot{y} = l_3 + J_3 \begin{bmatrix} u_2 \\ u_4 \end{bmatrix} \quad (28)$$

where

$$l_3 = \begin{bmatrix} -\cos(\psi)\alpha^2 x_3^3 - 3\sin(\psi)\alpha x_3 x_4 \\ -\sin(\psi)\alpha^2 x_3^3 + 3\cos(\psi)\alpha x_3 x_4 \end{bmatrix} \quad (29)$$

and J_3 is the new decoupling matrix:

$$J_3 = \begin{bmatrix} -\sin(\psi)x_3^2 & \cos(\psi) \\ \cos(\psi)x_3^2 & \sin(\psi) \end{bmatrix} \quad (30)$$

We are now able to decouple the two equations because J_3 is full rank, except in the case where the bicycle's velocity, x_3 , is zero. The relative degree of each output equation is 3 so the relative degree of the system is 6, which equals the order of the system. Therefore, there are no internal dynamics.

We can now solve for the control input, $\hat{u} \triangleq [u_2, u_4]^T$. Let the synthetic input, v_{FL} , be defined as follows:

$$v_{FL} = \ddot{y} \quad (31)$$

We assume that we know the desired trajectory of the bicycle ($x_{1d}(t), x_{2d}(t)$) and can differentiate it freely. We chose a simple tracking control law:

$$\left(\frac{d}{dt} + \lambda_1\right)^3 \varepsilon_1 = 0 \quad (32)$$

$$\left(\frac{d}{dt} + \lambda_2\right)^3 \varepsilon_2 = 0 \quad (33)$$

where λ_1 and λ_2 are the strictly positive constants and ε_1 and ε_2 are the differences between the actual trajectory and the desired trajectory, specifically $\varepsilon_1 = x_1 - x_{1d}$ and $\varepsilon_2 = x_2 - x_{2d}$. We can now write an explicit expression for \hat{u} :

$$\hat{u} = J_3^{-1}(v_{FL} - l_3) \quad (34)$$

where l_3 and J_3 are defined in Eqs. (29) and (30), and

$$v_{FL} = \begin{bmatrix} \ddot{x}_{1d} - 3\lambda_1\dot{\varepsilon}_1 - 3\lambda_1^2\varepsilon_1 - \lambda_1^3\varepsilon_1 \\ \ddot{x}_{2d} - 3\lambda_2\dot{\varepsilon}_2 - 3\lambda_2^2\varepsilon_2 - \lambda_2^3\varepsilon_2 \end{bmatrix} \quad (35)$$

4 Dynamic Surface Control

In this section, we describe the design of a dynamic surface controller to control the extended-state uncertain system, which is written as

$$\dot{x}_1 = \cos(\psi)x_3 + w_1 \quad (36)$$

$$\dot{x}_2 = \sin(\psi)x_3 + w_2 \quad (37)$$

$$\dot{\psi} = \alpha x_3 + w_3 \quad (38)$$

$$\dot{\alpha} = u_2 + w_4 \quad (39)$$

$$\dot{x}_3 = x_4 \quad (40)$$

$$\dot{x}_4 = u_4 \quad (41)$$

Here we have simply modified the extended-state equations, Eqs. (22)–(27), by adding disturbances (w_1, w_2, w_3 , and w_4) to the first four equations. We next present a method for defining states and state-dependent disturbances to transform the system into strict

feedback form. We then define the sliding surfaces and derive the control law.

4.1 Transformation into Strict Feedback Form. It is straightforward to use DSC if a system is in strict feedback form, as described in Ref. [5]. For a single-input single-output (SISO) system, strict feedback form is as follows:

$$\dot{z}_1 = z_2 + f_1(z_1) + \Delta f_1(z_1)$$

$$\dot{z}_2 = z_3 + f_2(z_1, z_2) + \Delta f_2(z_1, z_2)$$

\vdots

(42)

$$\dot{z}_{n-1} = z_n + f_{n-1}(z_1, \dots, z_{n-1}) + \Delta f_{n-1}(z_1, \dots, z_{n-1})$$

$$\dot{z}_n = f_n(z, \dots, z_n) + g_n(z, \dots, z_n)u + \Delta f_n(z, \dots, z_n)$$

where z_i are the states, $f_i(z_j, \dots, z_k)$ and $g_i(z_j, \dots, z_k)$ are the functions of states $z_j - z_k$, $\Delta f_i(z_j, \dots, z_j)$ are the model uncertainties, and u is the control input. As can be seen, the extended-state uncertain system in Eqs. (36)–(41) is not in strict feedback form.

To put the system in strict feedback form, we have developed a new method of defining new states and state-dependent disturbances. Since the bicycle has been modeled as a dual-input dual-output system, we consider the state equations in pairs. To form the first two state equations, Eqs. (36) and (37) are rewritten as

$$\dot{x}_1 = x_5 + w_1 \quad (43)$$

$$\dot{x}_2 = x_6 + w_2 \quad (44)$$

where $x_5 = \cos(\psi)x_3$ and $x_6 = \sin(\psi)x_3$. Note that w_1 and w_2 are the same disturbances as in Eqs. (36) and (37). We assume that they are bounded with $|w_1| \leq \delta_1$ and $|w_2| \leq \delta_2$, where δ_1 and δ_2 are known positive constants.

Then, x_5 and x_6 are differentiated to form the next two state equations:

$$\dot{x}_5 = x_7 + w_5 \quad (45)$$

$$\dot{x}_6 = x_8 + w_6 \quad (46)$$

where

$$x_7 = -\sin(\psi)\alpha x_3^2 + \cos(\psi)x_4 \quad (47)$$

$$x_8 = \cos(\psi)\alpha x_3^2 + \sin(\psi)x_4 \quad (48)$$

$$w_5 = -\sin(\psi)x_3 w_3 \quad (49)$$

$$w_6 = \cos(\psi)x_3 w_3 \quad (50)$$

Note that w_5 and w_6 are state-dependent disturbances. We assume that w_3 , from Eq. (38), is bounded with $|w_3| \leq \delta_3$, where δ_3 is a known positive constant. Assuming we have access to the state, we can compute the uncertainty bounds, δ_5 and δ_6 , for w_5 and w_6 , respectively:

$$|w_5| \leq |\sin(\psi)x_3\delta_3| = \delta_5 \quad (51)$$

$$|w_6| \leq |\cos(\psi)x_3\delta_3| = \delta_6 \quad (52)$$

Since x_3 and ψ change over time, the uncertainty bounds change over time and must be recomputed at each time step. Since this is a physical system, x_3 will never be infinite, so δ_5 and δ_6 will never be infinite.

Finally, x_7 and x_8 are differentiated to form the final two state equations, in which u_2 and u_4 explicitly appear:

$$\dot{x}_7 = -\cos(\psi)\alpha^2 x_3^3 - 3\sin(\psi)\alpha x_3 x_4 - \sin(\psi)x_3^2 u_2 + \cos(\psi)u_4 + w_7 \quad (53)$$

$$\dot{x}_8 = -\sin(\psi)\alpha^2 x_3^3 + 3 \cos(\psi)\alpha x_3 x_4 + \cos(\psi)x_3^2 u_2 + \sin(\psi)u_4 + w_8 \quad (54)$$

where

$$w_7 = -(\cos(\psi)\alpha x_3^2 + \sin(\psi)x_4)w_3 - \sin(\psi)x_3^2 w_4 \quad (55)$$

$$w_8 = -(\sin(\psi)\alpha x_3^2 - \cos(\psi)x_4)w_3 + \cos(\psi)x_3^2 w_4 \quad (56)$$

Again, w_7 and w_8 are state-dependent disturbances. We assume that w_4 , from Eq. (39), is bounded with $|w_4| \leq \delta_4$, where δ_4 is a known positive constant. Assuming we have access to the state, we can compute the uncertainty bounds, δ_7 and δ_8 , for w_7 and w_8 , respectively:

$$|w_7| \leq \max(|(\cos(\psi)\alpha x_3^2 + \sin(\psi)x_4)\delta_3 \pm \sin(\psi)x_3^2 \delta_4|) = \delta_7 \quad (57)$$

$$|w_8| \leq \max(|(\sin(\psi)\alpha x_3^2 - \cos(\psi)x_4)\delta_3 \pm \cos(\psi)x_3^2 \delta_4|) = \delta_8 \quad (58)$$

Again, since the states (x_3 , x_4 , ψ , and α) change over time, the uncertainty bounds change over time and must be recomputed at each time step. Since this a physical system, x_3 and x_4 will never be infinite, so δ_7 and δ_8 will never be infinite.

4.2 Sliding Surfaces and Control Law. Now we define sliding surfaces and derive the control law using the DSC design algorithm in Ref. [5]. Since the bicycle has been modeled as a dual-input dual-output system, we consider the sliding surfaces in pairs. As stated previously, we assume that we know the desired trajectory of the bicycle ($x_{1d}(t)$, $x_{2d}(t)$) and can differentiate it freely. As the goal is to send x_1 to x_{1d} and x_2 to x_{2d} , we define the first two sliding surfaces, S_1 and S_2 , to be

$$S_1 = x_1 - x_{1d} \quad (59)$$

$$S_2 = x_2 - x_{2d} \quad (60)$$

The sliding condition is

$$S_1 \dot{S}_1 \leq -k_1 S_1^2 \quad (61)$$

$$S_2 \dot{S}_2 \leq -k_2 S_2^2 \quad (62)$$

where k_1 and k_2 are the positive control gains. Taking derivatives of S_1 and S_2 , we find

$$\dot{S}_1 = \dot{x}_1 - \dot{x}_{1d} = x_5 + w_1 - \dot{x}_{1d} \quad (63)$$

$$\dot{S}_2 = \dot{x}_2 - \dot{x}_{2d} = x_6 + w_2 - \dot{x}_{2d} \quad (64)$$

Unfortunately, we cannot arbitrarily choose x_5 and x_6 to satisfy the sliding condition because the control does not explicitly appear in the equations for x_5 and x_6 . Therefore, we define synthetic inputs, \bar{x}_5 and \bar{x}_6 , as follows:

$$\bar{x}_5 = \dot{x}_{1d} - (k_1 + \delta_1)S_1 \quad (65)$$

$$\bar{x}_6 = \dot{x}_{2d} - (k_2 + \delta_2)S_2 \quad (66)$$

Here, the uncertainty bounds, δ_1 and δ_2 , are added to the control gains, k_1 and k_2 , to compensate for the unknown disturbances, w_1 and w_2 .

Our goal is now to drive \bar{x}_5 to some desired state, x_{5d} , and \bar{x}_6 to some desired state, x_{6d} . The desired states are determined from first-order filters:

$$\tau_1 \dot{x}_{5d} + x_{5d} = \bar{x}_5 \quad (67)$$

$$\tau_2 \dot{x}_{6d} + x_{6d} = \bar{x}_6 \quad (68)$$

where τ_1 and τ_2 are the filter parameters.

To drive the synthetic inputs to their desired states, we define the next two sliding surfaces, S_3 and S_4 , as

$$S_3 = x_5 - x_{5d} \quad (69)$$

$$S_4 = x_6 - x_{6d} \quad (70)$$

The sliding condition is

$$S_3 \dot{S}_3 \leq -k_3 S_3^2 \quad (71)$$

$$S_4 \dot{S}_4 \leq -k_4 S_4^2 \quad (72)$$

where k_3 and k_4 are the positive control gains. Taking derivatives of S_3 and S_4 , we find

$$\dot{S}_3 = \dot{x}_5 - \dot{x}_{5d} = x_7 + w_5 - \dot{x}_{5d} \quad (73)$$

$$\dot{S}_4 = \dot{x}_6 - \dot{x}_{6d} = x_8 + w_6 - \dot{x}_{6d} \quad (74)$$

The control does not explicitly appear in the equations for x_7 and x_8 , so again we cannot arbitrarily chose x_7 and x_8 to satisfy the sliding condition. Therefore, we define synthetic inputs, \bar{x}_7 and \bar{x}_8 , as follows:

$$\bar{x}_7 = \dot{x}_{5d} - (k_3 + \delta_3)S_3 \quad (75)$$

$$\bar{x}_8 = \dot{x}_{6d} - (k_4 + \delta_4)S_4 \quad (76)$$

Again, the uncertainty bounds are added to the control gains to compensate for the unknown disturbances.

Our goal is now to drive \bar{x}_7 to some desired state, x_{7d} , and \bar{x}_8 to some desired state, x_{8d} . The desired states are determined from first-order filters:

$$\tau_3 \dot{x}_{7d} + x_{7d} = \bar{x}_7 \quad (77)$$

$$\tau_4 \dot{x}_{8d} + x_{8d} = \bar{x}_8 \quad (78)$$

where τ_3 and τ_4 are the filter parameters.

To drive the synthetic inputs to their desired states, we define the last two sliding surfaces:

$$S_5 = x_7 - x_{7d} \quad (79)$$

$$S_6 = x_8 - x_{8d} \quad (80)$$

The sliding conditions are

$$S_5 \dot{S}_5 \leq -k_5 S_5^2 \quad (81)$$

$$S_6 \dot{S}_6 \leq -k_6 S_6^2 \quad (82)$$

where k_5 and k_6 are the positive control gains. Taking derivatives of S_5 and S_6 , we find

$$\dot{S}_5 = \dot{x}_7 - \dot{x}_{7d} \quad (83)$$

$$\dot{S}_6 = \dot{x}_8 - \dot{x}_{8d} \quad (84)$$

Fortunately, the controls, u_2 and u_4 , appear in the equations for \dot{x}_7 and \dot{x}_8 , as shown in Eqs. (53) and (54), so we can solve for $\hat{u} = [u_2, u_4]^T$ to satisfy the sliding condition in Eqs. (81) and (82), which results in

$$\hat{u} = J^{-1}(v_{\text{DSC}} - l) \quad (85)$$

where

$$J = \begin{bmatrix} -\sin(\psi)x_3^2 & \cos(\psi) \\ \cos(\psi)x_3^2 & \sin(\psi) \end{bmatrix} \quad (86)$$

$$v_{\text{DSC}} = \begin{bmatrix} \dot{x}_{7d} - (k_5 + \delta_5)S_5 \\ \dot{x}_{8d} - (k_6 + \delta_6)S_6 \end{bmatrix} \quad (87)$$

$$l = \begin{bmatrix} -\cos(\psi)\alpha^2x_3^3 - 3\sin(\psi)\alpha x_3x_4 \\ -\sin(\psi)\alpha^2x_3^3 + 3\cos(\psi)\alpha x_3x_4 \end{bmatrix} \quad (88)$$

Note that we have added the uncertainty bounds, δ_7 and δ_8 , to the control gains to compensate for the unknown disturbances w_7 and w_8 .

Equation (85) is very similar to Eq. (34), the control law derived for the feedback linearization case. Specifically, we find $J = J_3$ and $l = l_3$. The difference is that the synthetic control v is now a function of the sliding surfaces, desired trajectories, control gains, and disturbance bounds.

There exists a set of control gains, k_i , and filter parameters τ_i such that the system is semiglobally stable [5]. A method for choosing control gains and filter parameters is presented in Ref. [19]; however, we have simply chosen k and τ through iteration, as explained in Sec. 5.2. For reasons also explained in Sec. 5.2, we impose control input bounds that lead to transient control input saturation, resulting in a controller that is locally stable but is not guaranteed to be semiglobally stable. While out of the scope of this paper, future work could explore including the control input bounds in the plant model and developing a controller that achieves semiglobal stability despite control input saturation.

5 Simulation and Results

5.1 Feedback Linearization. Simulations were carried out to test the performance of the feedback linearization controller in tracking a desired trajectory, which was chosen to be $x_{1d} = t$ and $x_{2d} = \sin(t) + t$. MATLAB's ordinary differential equation (ODE) solver *ode45* (with default options) was employed to solve Eqs. (22)–(27). Initial conditions were chosen as follows: $[x_{10}, x_{20}, \psi_0, \alpha_0, x_{30}, x_{40}] = [0.5, 2, 0.01, 0, 0.01, 0]$. The control inputs were forced to remain between -10 and 10 to ensure convergence of the ODE solver. This was achieved by using Eq. (34) to compute the desired value of the control and then equating the actual control to either the desired control, if the desired control was within the allowed range, or the closest bound (-10 or 10), if the desired control was outside of the allowed range.

Results of the simulation show that though the bicycle does not start on the desired trajectory, after an initial period of time it converges to and stays on the desired trajectory, for an appropriate choice of the parameter λ . Through iteration λ was chosen to be $\lambda = [\lambda_1, \lambda_2]^T = [5, 5]^T$. For integer values of $\lambda_1 = \lambda_2 > 5$, the bicycle was unable to converge to the desired trajectory due to saturation of the control input. For integer values of $\lambda_1 = \lambda_2 < 5$, the bicycle converged to the trajectory more slowly than if $\lambda_1 = \lambda_2 = 5$. In the general case, the best choice of λ_1 and λ_2 is a function of the control input bounds.

To test the robustness of the feedback linearization controller, it was also used to control the uncertain system, Eqs. (36)–(41). For the purposes of simulation, the disturbances (unknown to the controller) included a static offset and a random component:

$$w_1 = 0.10 + 0.02r_1(t) \quad (89)$$

$$w_2 = 0.15 + 0.02r_2(t) \quad (90)$$

$$w_3 = 0.20 + 0.02r_3(t) \quad (91)$$

$$w_4 = 0.10 + 0.02r_4(t) \quad (92)$$

where $r_i(t) \sim \mathcal{N}(0, 1)$. Physically, these disturbances represent model uncertainty in addition to unknown forcing that affects the bicycle's velocity and its heading and steering angular velocities.

Results of the simulation are presented in Figs. 2 and 3. Figure 2 shows the tracking error in x_1 and x_2 . There exists a steady state error between the desired trajectory and the actual trajectory. More error exists in x_2 because the static offset chosen for w_2 was larger than that chosen for w_1 , as shown in Eqs. (89) and (90). It is clear from Fig. 2 that feedback linearization is unable to com-

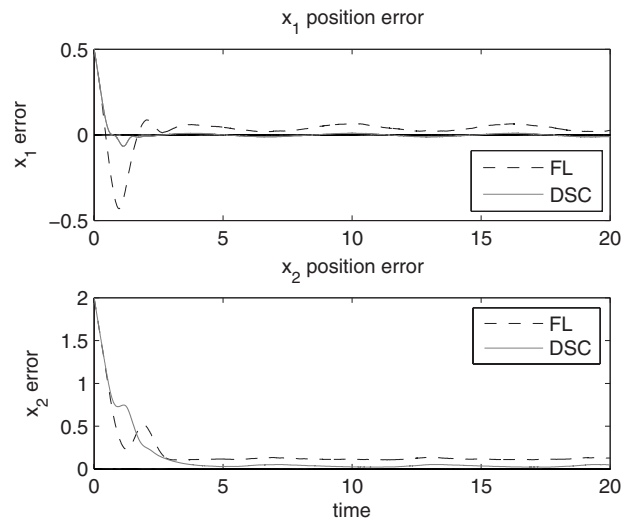


Fig. 2 Tracking error in x_1 and x_2 when MIMO FL and MIMO DSC are applied to the uncertain system

pensate for the disturbances that have been introduced.

Figure 3 shows control inputs u_2 (angular velocity) and u_4 (second derivative of velocity, or jerk). While the bicycle is finding the trajectory, the control input saturates. After converging to the trajectory, the inputs settle into a steady state pattern, which is oscillatory because of the sinusoidal nature of the desired trajectory. Figure 3 also includes an approximation of the desired forward velocity, u_1 , computed from u_4 using MATLAB's numerical integrator *trapz*. Note that since we control the forward velocity of

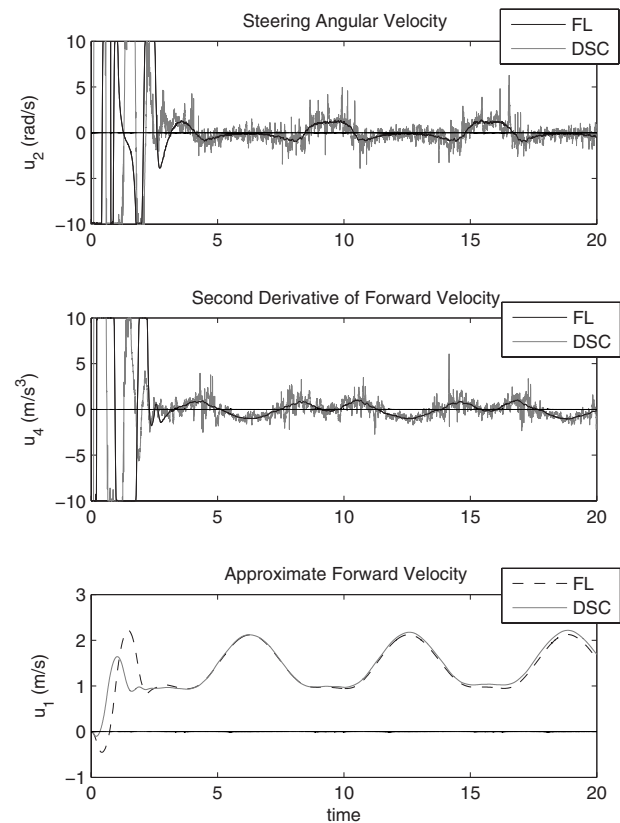


Fig. 3 Control inputs u_2 and u_4 and an approximation of u_1 (computed from u_4) when MIMO FL and MIMO DSC are applied to the uncertain system

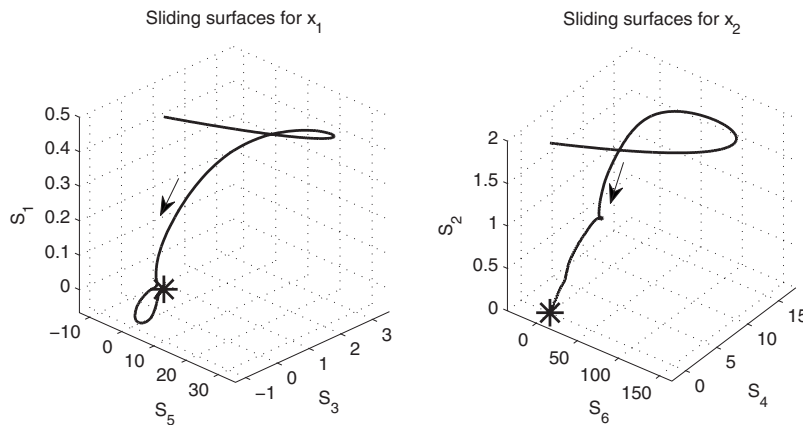


Fig. 4 Sliding surfaces for x_1 and x_2 . The stars indicate the point (0,0,0) and the arrows indicate the direction of increasing time. All surfaces converge to approximately zero.

the bicycle by specifying the bicycle's jerk, we have designed a dynamic controller. Applying this controller to a physical system would require integrating u_4 in real time. Numerical integration would lead to errors, which are not captured in this simulation.

As a result of Eq. (5), the physical values of the various inputs are related to the distance, L . For $L=1$ m, the maximum jerk is 10 m/s^3 , the maximum acceleration is $\sim 5 \text{ m/s}^2$ (or about 0.5 G), and the maximum forward velocity is $\sim 3 \text{ m/s}$ (or about 6.7 m/h) over the time period $t=0$ s to $t=20$ s. Expanding the allowable range for the inputs would increase the maximum jerk, acceleration, and velocity.

5.2 Dynamic Surface Control. Using DSC, we are able to reduce the steady state error that results when the uncertain system is controlled using feedback linearization. Simulations were performed to test the performance of the dynamic surface controller. The same desired trajectory and input bounds used in the feedback linearization case were used in the DSC case. Again, MATLAB's *ode45* was employed to solve the state equations, Eqs. (36)–(41), in addition to the four filter equations, Eqs. (67), (68), (77), and (78). Initial conditions for the state equations were chosen as follows: $[x_{1o}, x_{2o}, \psi_o, \alpha_o, x_{3o}, x_{4o}] = [0.5, 2, 0.01, 0, 0.01, 0]$. Initial conditions for the filter equations were computed from the initial conditions for the state equations. The uncertainty bounds δ_1 , δ_2 , and δ_4 were each assumed to be 0.2, and δ_3 was assumed to be 0.25. The uncertainty bounds δ_5 , δ_6 , δ_7 , and δ_8 , which change over time as a function of the state, were calculated at each iteration of the solver using Eqs. (51), (52), (57), and (58). Control gains $k=[k_1, k_2, \dots, k_6]$ and filter parameters $\tau=[\tau_1, \tau_2, \tau_3, \tau_4]$ were chosen by iteration. Up to a point, larger values of k_i lead to faster convergence of the bicycle to the desired trajectory. However, when the k_i s become too large, the bicycle is unable to converge to the desired trajectory due to saturation of the control input. Small values of τ_i lead to better tracking but high control action, while large values of τ_i lead to smoother control but more error.

The simulation was run using the disturbances in Eqs. (89)–(92). The values of the control gain were chosen to be $k=[10, 10, 1, 1, 10, 10]$, and the values of the filter parameter were chosen to be $\tau=[0.05, 0.05, 0.05, 0.05]$.

Results of the simulation are presented in Figs. 2–4. Figure 2 shows that the tracking error in the DSC case is significantly less than in the feedback linearization case. However, in the DSC case, the control inputs u_2 and u_4 exhibit high frequency control action in order to reject the disturbances, as can be seen in Fig. 3. Numerically integrating u_4 smoothes the plot of u_1 . Figure 4 shows

the behavior of the three sliding surfaces for x_1 and the three sliding surfaces for x_2 . Each sliding surface converges to approximately zero during the simulation.

This simulation was rerun with several different values for the additive disturbances. While the dynamic surface controller was able to converge for disturbances with large static offsets, the differential equation solver had trouble converging for disturbances with large random components. When the solver was able to converge, increasing the random component of the disturbances increased the control action required for trajectory following.

6 Conclusions

DSC, a robust nonlinear control technique, is generally applied to mismatched systems in strict feedback form. In this paper, we describe a new method of defining states and state-dependent disturbances that allowed us to transform a nonlinear mismatched dynamic system into strict feedback form. The method developed here could be used for other mismatched dynamic systems requiring robust nonlinear control.

We applied this method to a MIMO extended-state kinematic model of a bicycle, which originally was not in strict feedback form. After the system was transformed into strict feedback form, we were able to design a dynamic surface controller. We compared the performance of the dynamic surface controller to that of a controller designed using feedback linearization.

Both feedback linearization and DSC performed well when controlling the disturbance-free bicycle model. However, when disturbances are added, the feedback linearization controller was unable to track the desired trajectory. Instead, a steady state error, the magnitude of which was a function of the magnitude of the additive disturbance, existed between the actual and desired trajectory. The dynamic surface controller was able to reject the additive disturbance and track the desired trajectory. However, significant control action was required. By increasing the DSC filter parameter, τ , the control became smoother but tracking error increased. This demonstrates the trade-off between control action and tracking error in all sliding controllers.

Acknowledgment

The authors would like to thank Hope Weiss for her helpful comments. J.L.M. was funded by a NDSEG fellowship.

References

- [1] Slotine, J. E., and Li, W., 1991, *Applied Nonlinear Controls*, Prentice-Hall, Englewood Cliffs, NJ.

- [2] Krstić, M., Kanellakopoulos, I., and Kokotović, P., 1995, *Nonlinear and Adaptive Control Design*, Wiley, New York.
- [3] Won, M., and Hedrick, J. K., 1996, "Multiple-Surface Sliding Control of a Class of Uncertain Nonlinear Systems," *Int. J. Control*, **64**(4), pp. 693–706.
- [4] Swaroop, D., Hedrick, J. K., Yip, P. P., and Gerdes, J. C., 2000, "Dynamic Surface Control for a Class of Nonlinear Systems," *IEEE Trans. Autom. Control*, **45**(10), pp. 1893–1899.
- [5] Gomes, R. M. F., Sousa, J. B., and Pereira, F. L., 2003, "Integrated Maneuver and Control Design for ROV Operations," *Proc. IEEE OCEANS 2003*, Vol. 2, pp. 703–710.
- [6] Lu, X. Y., Tan, H. S., Shladover, S., and Hedrick, J. K., 2001, "Nonlinear Longitudinal Controller Implementation and Comparison for Automated Cars," *ASME J. Dyn. Syst., Meas., Control*, **123**(2), pp. 161–167.
- [7] Girard, A., and Hedrick, J. K., 2001, "Dynamic Positioning of Ships Using Nonlinear Dynamic Surface Control," *Proceedings of the Fifth IFAC Symposium on Nonlinear Control Systems 2001*.
- [8] Yao, B., and Tomizuka, M., 1997, "Adaptive Robust Control of SISO Nonlinear Systems in a Semi-Strict Feedback Form," *Automatica*, **33**, pp. 893–900.
- [9] Yao, B., and Tomizuka, M., 2001, "Adaptive Robust Control of MIMO Nonlinear Systems in Semi-Strict Feedback Forms," *Automatica*, **37**, pp. 1305–1321.
- [10] Getz, N., and Marsden, J., 1995, "Control for an Autonomous Bicycle," *Proceedings of IEEE Conference on Robotics and Automation 1995*, Vol. 2, pp. 1397–1402.
- [11] Lee, S., and Ham, W., 2002, "Self Stabilizing Strategy in Tracking Control of Unmanned Electric Bicycle With Mass Balance," *Proceedings of IEEE/RSJ Conference on Intelligent Robots and Systems 2002*, Vol. 3, pp. 2200–2205.
- [12] Astrom, K., Klein, R., and Lennartsson, A., 2005, "Bicycle Dynamics and Control: Adapted Bicycles for Education and Research," *IEEE Control Syst. Mag.*, **25**(4), pp. 26–47.
- [13] Peng, H., and Tomizuka, M., 1990, "Vehicle Lateral Control for Highway Automation," *Proceedings of American Control Conference 1990*, pp. 788–794.
- [14] Hedrick, J. K., Tomizuka, M., and Varaiya, P., 1994, "Control Issues in Automated Highway Systems," *IEEE Control Syst. Mag.*, **14**(6), pp. 21–32.
- [15] Mathieu, J. L., and Hedrick, J. K., 2010, "Robust Multivariable Dynamic Surface Control for Position Tracking of a Bicycle," *Proceedings of the American Control Conference 2010*, ACC-201-WeB11.1, pp. 1159–1165.
- [16] Iuchi, K., Niki, H., and Murakami, T., 2005, "Attitude Control of Bicycle Motion by Steering Angle and Variable COG Control," *Proceedings of IEEE IECON 2005*, pp. 2065–2070.
- [17] Isidori, A., 1995, *Nonlinear Control Systems*, Springer, New York.
- [18] Sastry, S., 1999, *Nonlinear Systems: Analysis, Stability, and Control*, Springer, New York.
- [19] Song, B., Hedrick, J. K., and Howell, A., 2002, "Robust Stabilization and Ultimate Boundedness of Dynamic Surface Control Systems via Convex Optimization," *Int. J. Control*, **75**(12), pp. 870–881.